Prepared for submission to JINST

The PANDA Endcap Disc DIRC

K. Föhl,[c,1] **A. Ali,**[a] **A. Belias,**[a] **R. Dzhygadlo,**[a] **A. Gerhardt,**[a] **K. Götzen,**[a] **G. Kalicy,**[a] **M. Krebs,**[a] **D. Lehmann,**[a] **F. Nerling,**[a] **M. Patsyuk,**[a] **K. Peters,**[a] **G. Schepers,**[a] **L. Schmitt,**[a] **C. Schwarz,**[a] **J. Schwiening,**[a] **M. Traxler,**[a] **M. Böhm,**[b] **W. Eyrich,**[b] **A. Lehmann,**[b] **M. Pfaffinger,**[b] **F. Uhlig,**[b] **M. Düren,**[c] **E. Etzelmüller,**[c] **A. Hayrapetyan,**[c] **K. Kreutzfeld,**[c] **O. Merle,**[c] **J. Rieke,**[c] **M. Schmidt**[c] **T. Wasem,**[c] **P. Achenbach,**[d] **M. Cardinali,**[d] **M. Hoek,**[d] **W. Lauth,**[d] **S. Schlimme,**[d] **C. Sfienti,**[d] **M. Thiel,**[d]

[a] *GSI Helmholtzzentrum für Schwerionenforschung GmbH, Planckstraße 1, 64291 Darmstadt, Germany*

[b] *Physikalisches Institut, Friedrich-Alexander-Universität Erlangen-Nürnberg, Erwin-Rommel-Str. 1, 91058 Erlangen, Germany*

[c] *II. Physikalisches Institut, Justus-Liebig-Universität Gießen, Heinrich-Buff-Ring 16, 35392 Gießen, Germany*

[d] *Institut für Kernphysik, Johannes Gutenberg-Universität Mainz, Johann-Joachim-Becher-Weg 45, 55128 Mainz, Germany*

E-mail: klaus.foehl@exp2.physik.uni-giessen.de

Abstract: Positively identifying charged kaons in the PANDA forward endcap solid angle range can be achieved with the Endcap Disc DIRC, allowing kaon-pion separation from 1 up to 4 GeV/c with a separation power of at least 3 standard deviations. Design, performance, and components of this DIRC are given, including the recently introduced TOFPET-ASIC based read-out. Results of a prototype operated in a test beam at DESY in 2016 are shown.

[1] Corresponding Author

Contents

1 Introduction

A key feature of the FAIR laboratory will be new experimental infrastructure. Its construction has recently started and will expand the current GSI facilities at Darmstadt. The antiproton PANDA experiment [1] features among the day one infrastructure items of FAIR and is to be located on the HESR storage ring, which holds a continuous stored 1.5 to 15 GeV/c antiproton beam. Electron cooling is provided for antiproton momenta of up to 8.9 GeV/c. Being a fixed-target experiment, PANDA (Fig. 1) will mainly use proton targets in the form of either gas jet target or pellet target. The gas jet target can also be operated with noble gases. The four physics pillars for the PANDA experiment are hadron spectroscopy in the charm-quark range, nucleon structure, hadrons in matter, and exotic nuclei [2].

Excellent Particle Identification (PID) is crucial for the abovementioned physics topics. The Endcap Disc DIRC (EDD) addresses the positive PID of charged kaons [3]). Being a Cherenkov detector of the DIRC type [4], the EDD is part of the PANDA target spectrometer (TS) and covers the PANDA forward endcap range of polar angles $\theta < 22^\circ$ while not obstructing particles in the elliptical phase space $\theta_X \times \theta_Y = 10^\circ \times 5^\circ$ continuing into the PANDA forward spectrometer (FS).

2 Requirements for the EDD

The EDD has to meet stringent boundary conditions. Geometrically there is little available space between forward electromagnetic calorimeter (EMC) and the housing of the PANDA solenoid. In terms of radiation length only a thin layer is allowed upstream of the EMC crystals. In particular the central parts of the EDD receive an important radiative load, less so the outer parts at polar

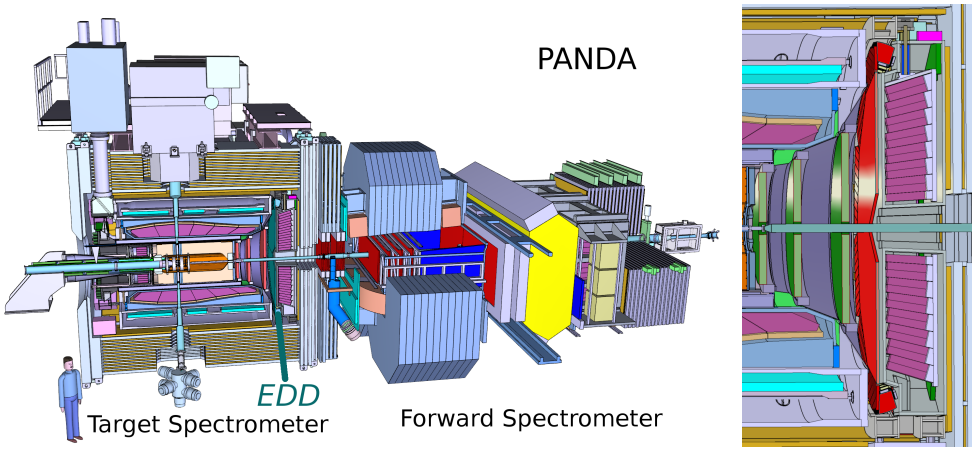

Figure 1. Cut-out side view of the PANDA experiment, left the onion-like part of the target spectrometer and right the individual stations of the forward spectrometer. The detail view far right shows the EDD with its optical components shown in red fitting tightly into the scarce available space, with some holding structures and cable paths upstream of the EDD not shown.

angles $\theta > 22°$, due to a combination of fixed target kinematics and the shielding effect from the central EMC. For the envisaged MCP-PMT sensors both the high magnetic field of about one tesla and the required lifetime expressed in collected anode charge need to be addressed.

Positive PID for charged kaons is the goal. For a Cherenkov detector which the EDD is the onset of Cherenkov radiation is a lower bound, and the onset of light transmission courtesy of total internal reflection determines the actual lower limit of the momentum range. The decreasing difference between kaon and pion Cherenkov angle for increasing momentum determines the upper limit of the momentum range.

In PANDA we expect a high interaction rate (luminosity up to $2{\cdot}10^{32}$ cm^{-2}s^{-1}) at the Interaction Point (IP) but multiplicities of the primary vertices at the IP of only 1.0±0.8 (at 2 GeV/c) to 2.3±1.8 (at 15 GeV/c) charged particles into the whole EDD active area [5]. An acceptable design should provide kaon-pion separation at 3 standard deviations (s.d.) for 4 GeV/c particles. It is desirable that the EDD system can contribute to the Online Trigger [6].

3 Gross EDD properties

The proposed EDD design (Fig. 2) has to fit a 2919 mm inscribing diameter, and depending on location there are 42 to 242 mm clearance in z direction [7]. The EDD system has 4 quadrants which can be mounted individually into the mechanical support structure of holding cross and holding plate. We anticipate ≈450 kg gross weight including holding structures and ≈85 kg weight per individual quadrant.

4 Simulated performance

Fig. 3 shows the expected performance obtained by Monte-Carlo simulations [6] done within the PANDA-Root framework [8]. At the IP positively charged kaons and pions of 4 GeV/c are emitted

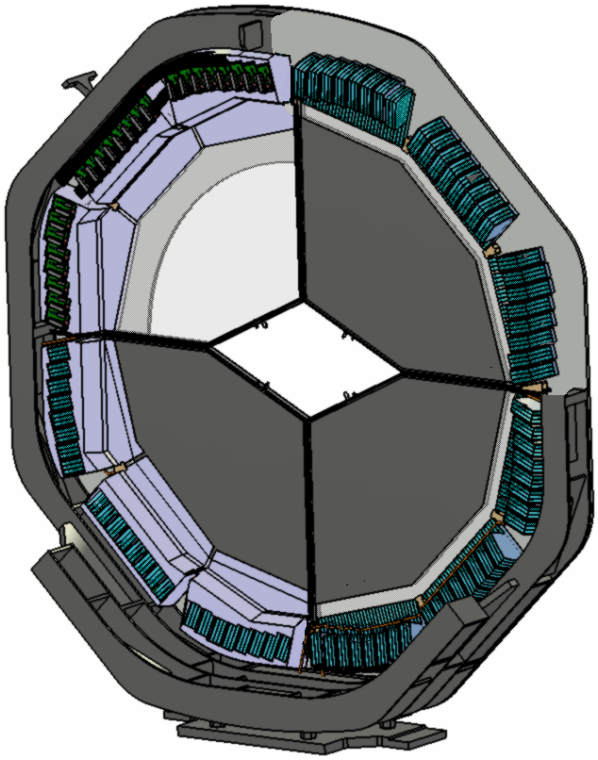

Figure 2. Partial cut-away figure of the EDD seen from the downstream side. Going clockwise starting at the top, one initially sees the EDD holding plate (light grey), the radiator (dark grey) and the optical components of the readout modules. Added subsequently are the EMC-EDD common holding frame (dark grey), then the ROM boxes (light violet), and finally electronics PCB boards plus cabling.

with directions forming an equidistant grid in $\tan\theta_X$ and $\tan\theta_Y$ space, numbers being 500 particles per particle type and grid point. They are tracked through the full PANDA magnetic field. The space between IP and EDD, however, is not populated with PANDA detector components. Wavelength-dependent optical transmission properties have been implemented for all the optical components. The MCP-PMT sensor was modelled with a blue sensitive photocathode plus dielectric LongPass $\lambda > 355$nm filter at the entrance window. Under best conditions (normal incidence of light on read-out units) one achieves $\sigma = 3.45$ mrad single photon resolution (SPR).

The Cherenkov photon hit patterns of particles arriving at the radiator plate were analysed using a log-likelihood method including position and timing information. The available tracking resolution from the upstream PANDA tracking stations was assumed to be 1 mrad.

The kaon-pion separation power values in figure 3 are shown as colour coded values and given in s.d. units. The use of a nearest neighbour display algorithm results in a chess board-like pattern. Due to the spiral tracks in the PANDA solenoid field this pattern which originates from the upright grid at the IP is rotated. The performance decrease when charged particle tracks get nearer to the readout faces (here the 3 polygon sides top right) has been described previously [9]. For constant θ value one notices a small difference in the performance fall-of near the horizontal and vertical sides, where photons can be internally reflected off the polished radiator side surface. This is

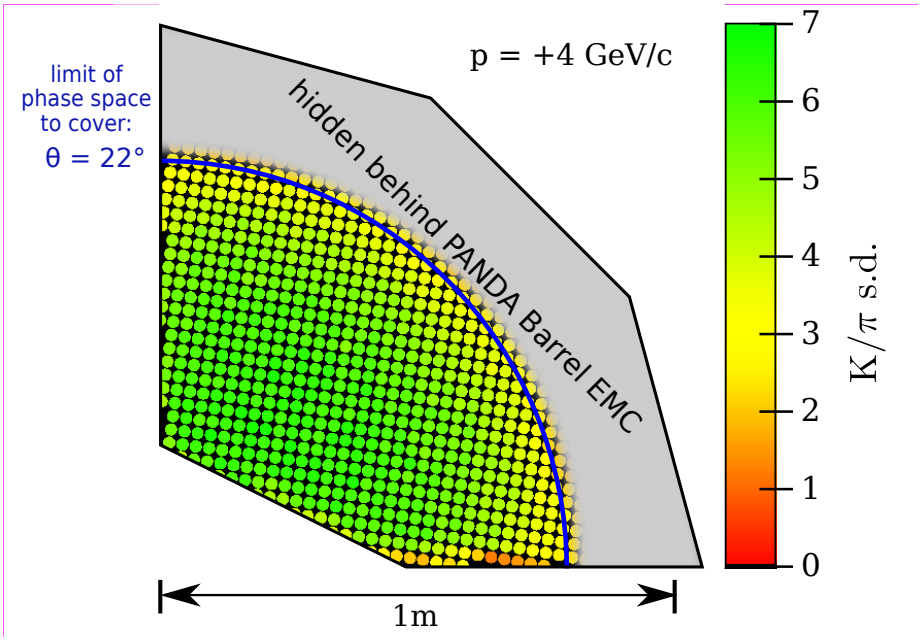

Figure 3. Monte-Carlo performance simulation of an EDD quadrant using the PANDA-Root framework. Positively charged kaons and pions of 4 GeV/c momentum originating at the IP are tracked through a realistic PANDA magnetic field but do not cross any material upstream of the EDD. The separation power is given in s. d. units, values are colour-coded. Tracking information from upstream units is assumed to have 1 mrad accuracy. For polar angles larger than 22° the performance values have been greyed out, as material from PANDA-subsystems that shield parts of the EDD like the Barrel EMC was not included in these simulations.

due to the saggital direction component of the charged particle tracks which makes the direct and reflected smiles from the Cherenkov photon pattern overlay for particles arriving near but not on the horizontal side. Near the vertical side such overlay does not occur for the simulated positively charged particles. Comparing horizontal and vertical sides an enhancement of the separation performance can be observed near the vertical edge. Apart from this detail the performance is rather similar to the B = 0 tesla case.

Except for small areas of edge effects the results from the Monte-Carlo simulations meet or exceed 3 s.d. separation power for 4 GeV/c particles inside the phase space of $\theta < 22°$ the EDD needs to cover.

5 Optical design and read-out

The EDD design comprises 4 quadrants that are optically not coupled. For the material of the optical components as shown in figure 4 one has to use synthetic amorphous fused silica (quartz glass or in short quartz) for transparency and radiation hardness reasons.

Each of the 4 radiator discs fits into a $1050 \times 1050 \times 20$ mm^3 box. Due to mechanical and manufacturing reasons the inside facing side is not curved but tangent on the elliptical phase space opening, hence the minimum polar angle covered is 6°. On each of the outward-facing radiator disc sides attaches a battery of 8 Readout Modules (ROM). Each ROM housing contains 3 readout units,

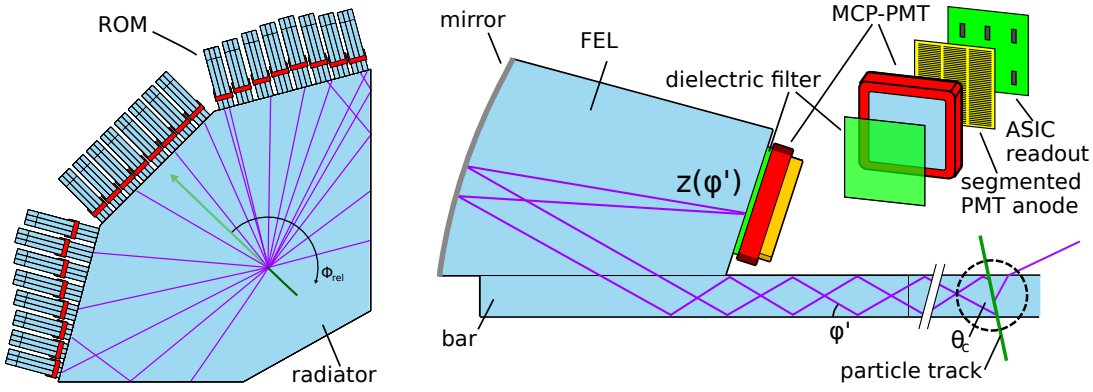

Figure 4. Radiator (left), ROM with bar and FEL (middle), and schematic filter plus sensor plus read-out package (right). The MCP-PMT pixels are physically or logically grouped into three vertical columns that optically match the three bar-plus-FEL units per ROM.

each 16 mm wide and formed of a quartz bar and a quartz Focussing Element (FEL) mechanically and optically coupled by optical contact bonding which is crucial because of the shallow angles of the photons crossing the seam. A thin air gap separates the readout units.

The mirror-coated cylindrical surface of each FEL focusses the photons on the photocathode of an MCP-PMT. As the Cherenkov photons cross the dielectric filter at close to 90° Angle of Incidence (AoI) one can use a standard Long Pass filter dielectric stack design for the specified $\lambda > 355$ nm transmission wavelength range.

Each ROM is read out by one MCP-PMT sensor with a square housing of 60 mm side length. Prototypes have been obtained from two companies which offer anode readout segmented into 100×3 or 128×6 pixels, logically grouped into 3 columns of pixels $\approx 0.5 \times 17$ mm^2 in pitch matching the readout unit's pitch. Over the PANDA lifetime these MCP-PMTs have to withstand the anticipated 7 C/cm^2 integrated anode charge.

For one EDD quadrant one requires 24 ROMs, 24 MCP-PMTs and 72 FELs. For the full detector of four quadrants one requires 96 ROMs, 96 MCP-PMTs and 288 FELs.

6 Readout system

On average one expects 21.2 detected Cherenkov photons per particle. A readout system based on the TOFPET ASIC is foreseen, to cope with the expected peak rate of 75 kHz per pixel.

The free-running hence self-triggering TOFPET system [10] consists of a sequence of PCBs. Board A accepts 128 channels into 2 TOFPET ASICs packaged together. Eight of such boards A are mezzanine to a board D, where an FPGA processes the signals from the incoming 1024 channels (and possibly from further daisy-chained D boards). The outgoing data is transferred onwards with a micro-HDMI cable. A fan-out box then accepts up to 12 cables to connect with the PC-housed interface card.

The photo of figure 5 shows boards A and D as they have been used in the electronics setup of the DESY 2016 test beam experiment.

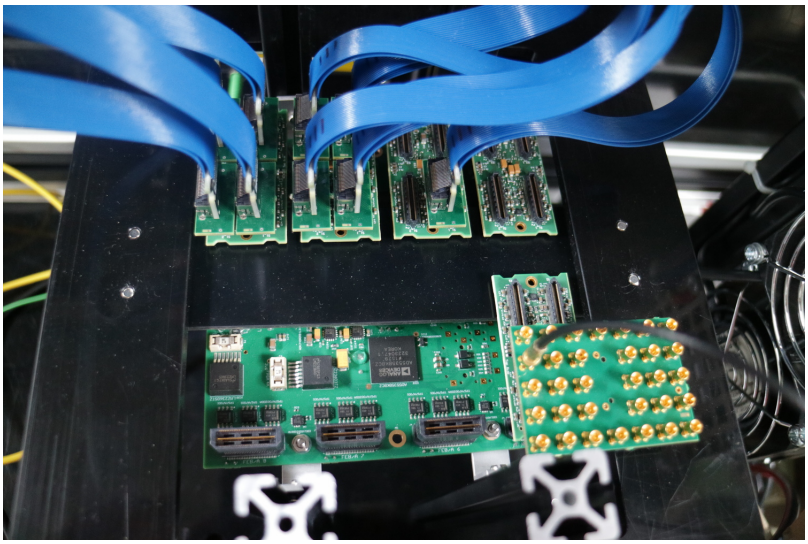

Figure 5. Ribbons of coaxial cables from the MCP-PMTs enter via custom adapter boards into the small TOFPET A boards holding the TOFPET ASICs. At the bottom about one half of the TOFPET D board with three open connectors (out of 8) can be seen. The trigger counters signal arrives bottom right.

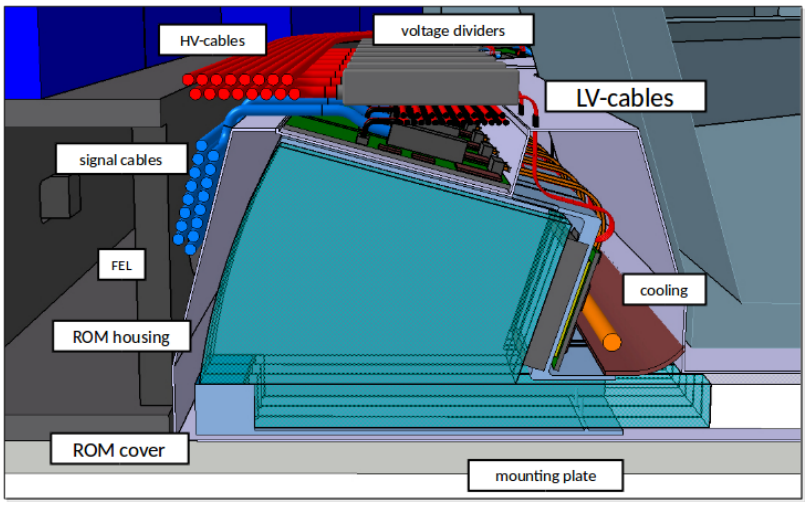

Figure 6. Cutaway view showing the geometry of the quartz optical components inside a ROM and the limited space available to the tighly arranged electronics and cable paths around it. The radiator plate attaches from the right, left in dark grey is the holding frame common to DIRC and TS Forward EMC, and light grey top right the allocated space for insulation and contents of said EMC.

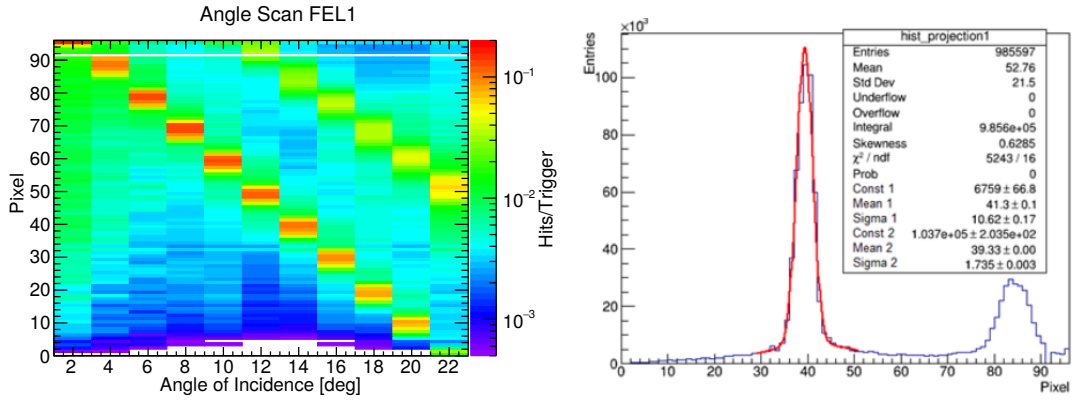

Figure 7. Angle scan (left) and intensity histogram for an Angle-of-Incidence of 14° (right) for the centre MCP-PMT column (receiving photons from the middle focussing element, labelled FEL 1). The weaker intensity peaks are photons that were reflected off the radiator bottom side. The electron beam crossed the radiator at 453.9 mm distance from the radiator-bar seam.

While the electronics circuit arrangement of the test beam experiment, suitably scaled up, would already be usable for the EDD, the boards A and D still need to be redesigned to fit the tight available volumina in the EDD shown in figure 6. One also needs to house cables, cooling and clean gas provision pipes in there.

7 DESY 2016 test beam

An EDD prototype of smaller size consisting of a $500 \times 500 \times 20\,\mathrm{mm}^3$ quartz radiator plate on loan from Nikon[1] and allowing to attach up to 5 ROMs to one radiator side [7] has been used in a test beam experiment at the T24 beamline of DESY in October 2016. A standard TOFPET system was complemented with custom PCBs and cabling to allow the readout of MCP-PMTs connected to ROMs inside the prototype housing [11].

Due to delivery issues only one fully FEL-filled ROM was available, which was connected to a Photonis MCP-PMT. The 3 GeV/c electron beam was collimated $5 \times 5\,\mathrm{mm}^2$ and $15 \times 15\,\mathrm{mm}^2$ upstream and downstream of the concrete shielding, respectively, and local wisdom indicated a spatial uncertainty of $\approx$5 mm and an angular uncertainty of $\approx$1 mrad on the radiator. The signals coincidence of two plastic scintillator finger counters and an electromagnetic calorimeter crystal (the latter plus lead shielding in front with a hole allowing to harden the beam), fed into an ancillary TOFPET channel, provided a software trigger and timing reference signal.

The results are from the middle (labelled FEL 1) of the three readout units, which feature different optical couplings between bar and FEL. Connection to the radiator plate and the MCP-PMT was with St. Gobain BC630 optical grease which did not introduce any wavelength-dependent optical filtering.

[1]Nikon Corporation Glass Business Unit, 10-1, Asamizodai 1-chome, Minami-ku, Sagamihara-city, Kanagawa 252-0328 Japan

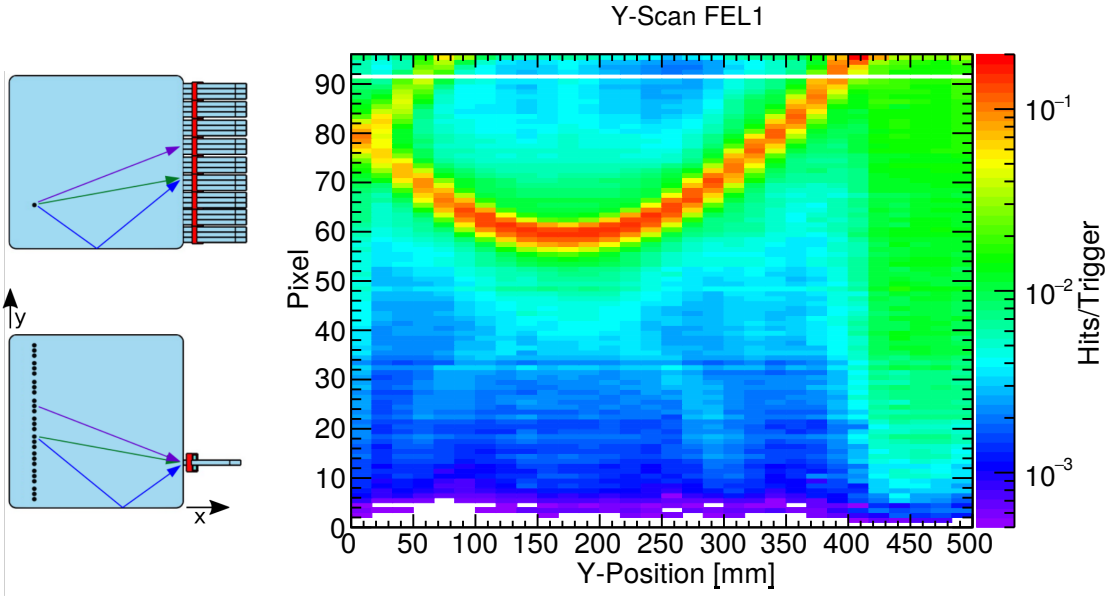

Figure 8. Experimental simulation of the expected EDD pattern with the Combined Events method combining photons from different runs into one event. The cartoon on the left shows the equivalence of photon paths from one beam position into an array of readout units to photons emitted along scan positions on a vertical line into a single readout unit. The beam position was at 347 mm distance from the radiator side connected to the optical readout.

For 14 degrees AoI figure 7 right shows position measurements with the MCP-PMT of direct photons and photons reflected off a radiator edge. For the readout unit the epoxy-glued bar-FEL seam gives a long pass edge filter effect at $\lambda = 295$ nm. The sigma of the distribution is 1.73 pixels or 0.86 mm which converts into 6.1 mrad angle resolution. This resolution value is dominated by the chromatic dispersion.

Taking a set of runs scanning the vertical beam position and reading one unit allows one to obtain a many-photon pattern which is the same as if there were one beam position but many readout units. Such a pattern is shown in figure 8. One can even experimentally simulate photon patterns from single particles in combining the event data from individual triggers, one from each vertical beam position to form one single combined event.

Figure 9 gives the Cherenkov angle histogram and the SPR values obtained from the combined events experimental data and the corresponding MC simulation. The average of 1.4 pixel hits per photon as observed in the 2016 DESY test beam was also incorporated into the MC simulations. The pixel hit multiplicity is 24.1 in the experiment and 25.7 in the MC simulation, the single photon resolution 7.57 mrad and 7.66 mrad, respectively.

With these combined events from different runs of a vertical scan set one creates a data sample which simulates the performance of a fully equipped prototype, analysing which one can obtain a histogram for the mean Cherenkov angle, a key number for the detector performance.

In order to discard background photons from contaminating the sample one averages over, a truncating mean-inspired algorithm was used discarting one by one outliers in angle until self-

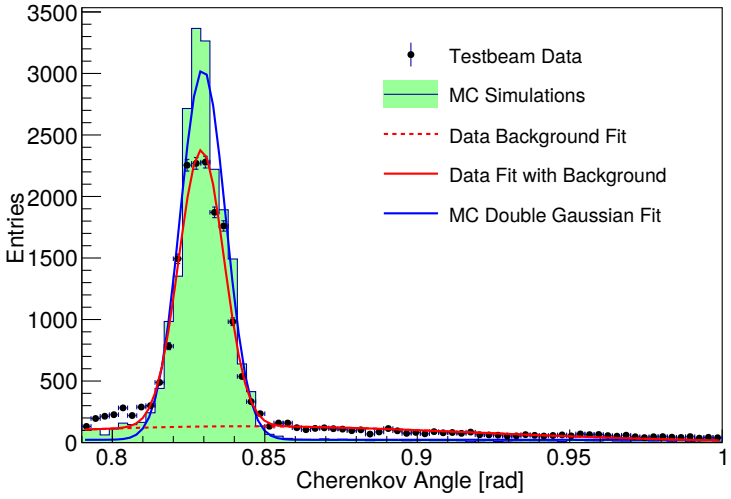

Figure 9. Histogram of single photon angle distribution, determined from the pixel hit distribution of vertical scan data runs. The beam position was at 347 mm distance from the radiator side connected to the optical readout. From a double Gaussian fit (red solid line) to the testbeam data (black data points) the main Gaussian curve (red solid line) gives $\sigma = 7.4$ mrad, to compare to the histogram of MC simulations (green filled area) with $\sigma = 7.6$ mrad (blue Gaussian fit).

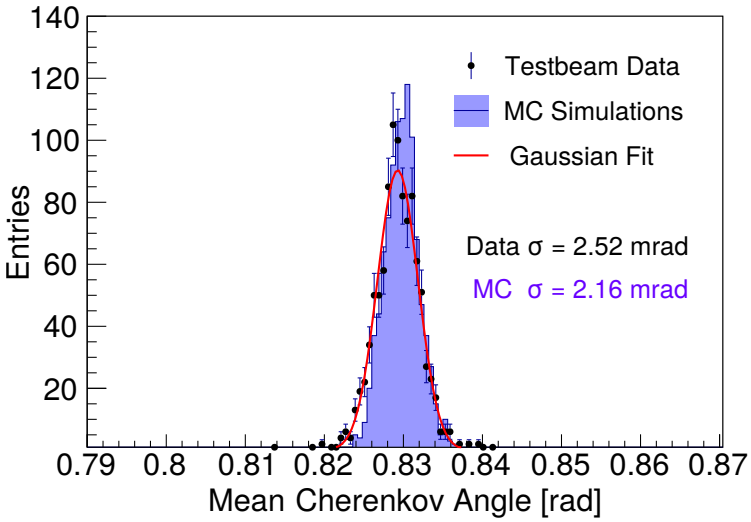

Figure 10. Reconstructed mean Cherenkov angle. From a series of runs with different vertical beam positions individual events were aggregated into combined events that reflect the performance of a prototype fully equipped with readout modules. The angle determined from testbeam data (black data points), the fit with a Gaussian curve (red solid line) giving $\sigma = 2.16$ mrad width, is compared to the histogram of MC simulations (violet filled area) and $\sigma = 2.52$ mrad.

consistency is reached in that all sample values are contained within its $\pm 3\sigma$ interval. The number of selected hits for this average are 12.8 for the data and 17.7 for the MC simulations.

Histograms of the mean Cherenkov angle from data and MC are shown in figure 10, the single photon resolutions are 2.52 mrad and 2.16 mrad, respectively.

8 Conclusions

An Endcap Disc DIRC detector prototype (which we feel is close to the design required for PANDA) with a TOFPET-based readout system was investigated in the DESY T24 test beam area using an electron beam of 3 GeV/c. The number of photons per charged particle track and the Cherenkov angle resolutions obtained from analysing the test beam data compare well with the results of Monte-Carlo simulation studies.

Acknowledgements

The authors would like to thank the DESY staff for their much appreciated help during the experiment time. The authors acknowledge financial support from the German funding agency BMBF and from the LOEWE programme HIC for FAIR.

References

[1] $\bar{\text{P}}$ANDA Collaboration, Technical Progress Report, FAIR–ESAC/Pbar 2005 http://www-panda.gsi.de/db/papersDB/PC19-050217_panda_tpr.pdf

[2] Felice Iazzi, *The PANDA Physics Program: Strangeness and more*, CETUP* 2015, 1743.050006.10.1063/1.4953307 (2016)

[3] M. Düren et al., *The Endcap Disc DIRC of PANDA*, Nucl. Instr. and Meth. A in press, doi:10.1016/j.nima.2017.02.077

[4] T. Kamae et al., *Focussing DIRC – A new compact Cherenkov ring imaging device*, Nucl. Instr. and Meth. A **382** (1996) 430

[5] A. Galoyan, V.V. Uzhinsky, *New Monte Carlo Implementation of Quark-Gluon-String model of* $\bar{\text{p}}$*p-Interactions* AIP Conference Proceedings 796, 2005, pp. 79–82.

[6] M. Schmidt et al., *Disc DIRC PID Algorithms*, these DIRC2017 proceedings

[7] E. Etzelmüller, *Developments towards the technical design and prototype evaluation of the PANDA Endcap Disc DIRC*, Dissertation JLU Giessen 2017

[8] Stefano Spataro for the PANDA collaboration, *The PandaRoot framework for simulation, reconstruction and analysis*, Journal of Physics: Conference Series 331 (2011) 032031, doi:10.1088/1742-6596/331/3/032031

[9] K. Föhl et al., *The focussing light guide disc DIRC design*, 2009 JINST 4 P11026, http://dx.doi.org/10.1088/1748-0221/4/11/P11026

[10] M. Rolo et al., *TOFPET ASIC for PET applications*, JINST 8 (2013) C02050

[11] J. Rieke, *Design of a compact photon detection system for the PANDA Disc DIRC*, Dissertation JLU Giessen 2017